ISSN 0915-633X

NATIONAL INSTITUTE FOR FUSION SCIENCE

A Tandem Parallel Plate Analyzer

Y. Hamada, A. Fujisawa, H. Iguchi, A. Nishizawa and
Y. Kawasumi

(Received - Oct. 17, 1996)

NIFS-460 Nov. 1996

RESEARCH REPORT
NIFS Series

NAGOYA, JAPAN

A Tandem Parallel Plate Analyzer

Y. Hamada, A. Fujisawa, H. Iguchi, A. Nishizawa and Y. Kawasumi

National Institute for Fusion Science

Nagoya, 464-01, Japan

ABSTRACT. By a new modification of a parallel plate analyzer the second-order focus is obtained in an arbitrary injection angle. This kind of an analyzer with a small injection angle will have an advantage of small operational voltage, compared to the Proca and Green analyzer where the injection angle is 30 degrees. Thus, the newly proposed analyzer will be very useful for the precise energy measurement of high energy particles in MeV range.

Keywords: analyzer, parallel plate analyzer, beam, HIBP

1. INTRODUCTION

The parallel plate electrostatic energy analyzer[1,2] is widely used in various fields of experimental physics and technology because of its simplicity and good focusing properties up to the second order in case of 30 degrees injection angle. It is also suited for the simultaneous multi-input-slit measurement of the energy of nearly parallel beams, since we can install many input-slit/detector sets utilizing the fact that the electric field is uniform.

In order to perform high-precision measurement of the energy of particles in MeV range by a parallel plate analyzer, the second-order focus is necessary and the injection angle must be 30 degrees. Then we have to apply a very high voltage of $V_a > (V_t \sin^2(\theta_{in}))/q_s$ to the upper parallel plate in order to bend the trajectory, where V_t is the energy of the particle and θ_{in} is the injection angle. q_s is the charge of the particle. In order to reduce the operational voltage, the injection angle must be reduced at the sacrifice of the second-order focus.

Here, we would like to propose a tandem parallel plate analyzer which has the second-order focus at any injection angle. By this analyzer, the multi-slit measurement of the precise change of the energy of several nearly parallel beams in MeV range may be more easily performed.

A heavy ion beam probe for the large plasma confinement machine, utilizes several MeV heavy ion beam and is required to measure the change of a few hundreds eV in the energy of the beam out of the plasma[3,4]. Since heavy ions like gold or thallium are used, a sector magnet for energy analysis may be larger than the confinement machine itself and very expensive. In addition, the multi-input-slit measurement by a sector magnet or electrostatic cylindrical deflector, to determine the wavelength of the turbulence in a plasma is very limited. This analyzer may be very useful to this kind of application.

2. ANALYZER MODEL AND THEORY

First, we discuss the aberration of a single parallel plate analyzer as shown in Fig. 1 (a). The basic equation of the trajectory (x, y) in the field free region after deflection by the uniform electric field is given by,

$$x = (h+y)\cot(\theta) + \frac{2.0V_t}{q_s E_p}\sin(2\theta), \tag{1}$$

where, (0, h) is position of the entrance slit of the analyzer as shown in Fig. 1(a). V_t is the energy of the particle and E_p is the electric field at the analyzer. The charge of the particle is q_s. θ is the injection angle to the analyzer

The aberration (δx) of a parallel plate analyzer at the focal point due to the change of the entrance angle to the analyzer ($\delta\theta$) is described by the following equation[2),

$$\delta x = \frac{4V_t}{q_s E_p}\frac{\cos(3\theta_1)}{\sin(\theta_1)}(\delta\theta)^2 - \frac{4V_t}{q_s E_p}\frac{\cos(2\theta_1)}{\sin^2(\theta_1)}(\delta\theta)^3, \tag{2}$$

where $\theta = \theta_1 + \delta\theta$ and θ_1 is the injection angle of the first-order focus. At $\theta_1 = 30°$, the second-order focus is obtained.

We discuss a model of a tandem parallel plate analyzer as shown in Fig. 1(b). The angle of a base plate (θ_s) is given by $\theta_s = \theta_1 + \theta_2$, where θ_1, θ_2 are the designed entrance angles to the first and second stages of a tandem analyzer respectively. The aberration of a tandem parallel plate analyzer can be calculated by the following equation of the straight trajectory after deflection by the second deflector,

$$x_1=\{L_t-h_1\cot(\theta)-\frac{2.0V_t}{q_sE_{p1}}\sin(2\theta)\}\frac{\sin(\theta)}{\sin(\theta_a)}+\frac{2.0V_t}{q_sE_{p2}}\sin(2\theta_a)+h_2\cot(\theta_a), \qquad (3)$$

where $\theta_a = \theta_s-\theta$. Other parameters are shown in Fig. 1(b). By a simple calculation, it is shown the terms of $L_t\frac{\sin(\theta)}{\sin(\theta_a)}$ and $h_1\cot(\theta)\frac{\sin(\theta)}{\sin(\theta_a)}$ are a linear function of $h_2\cot(\theta_a)$. Accordingly, we have three independent parameters of E_{p1}, E_{p2} and h_2, and we can find second-order focus at arbitrary angles of θ_1, θ_2 by the equations of $\frac{\delta x_1}{\delta\theta}=0$ and $\frac{\delta^2 x_1}{\delta\theta^2}=0$. The ratio of the electric fields under the parallel plates is given by the following equation after somewhat lengthy calculation,

$$\frac{\cos(3\theta_1)}{E_{p1}}=\frac{\cos(3\theta_2)}{E_{p2}}. \qquad (4)$$

The final aberration can be expressed in the following equation,

$$\delta x_1=\frac{4V_t}{q_sE_{p1}}\frac{\cos(2\theta_1)\sin(\theta_1)\cos(3\theta_2)-\cos(3\theta_1)\cos(3\theta_2)\sin(\theta_1+\theta_2)+\cos(3\theta_1)\sin(\theta_1)\cos(2\theta_2)}{\sin(\theta_1)\sin^2(\theta_2)}(\delta\theta)^3 . \qquad (5)$$

We can derive Eqs. (4) and (5) readily in the following way. We can assume without loss of generality that

$g(\theta_1)=0,\ \frac{\delta g(\theta)}{\delta\theta}=0$, at $\theta=\theta_1$ where $g(\theta)=L_t-h_1\cot(\theta)-\frac{2.0V_t}{q_sE_{p1}}\sin(2\theta)$, since $L_t\frac{\sin(\theta)}{\sin(\theta_a)}$ and $h_1\cot(\theta)\frac{\sin(\theta)}{\sin(\theta_a)}$ are a linear function of $h_2\cot(\theta_a)$. Then in the calculation of $\frac{\delta x_1}{\delta\theta}=0$ and $\frac{\delta^2 x_1}{\delta\theta^2}=0$ at Π_1, we can use Eq. (2) and more easily Equations (4) and (5) are obtained.

The focus point (x_{1f},h_{1f}) is given by,

$$x_{1f}=\frac{4V_t}{q_sE_{p2}}\sin(2\theta_2)\cos^2(\theta_2)-\left\{L_t-\frac{4V_t}{q_sE_{p1}}\sin(2\theta_1)\cos^2(\theta_1)\right\}\cos(\theta_s)-\left\{h_1-\frac{4V_t}{q_sE_{p1}}\cos(2\theta_1)\sin^2(\theta_1)\right\}\sin(\theta_s) \tag{6}$$

,

$$h_{1f}=\frac{4V_t}{q_sE_{p2}}\cos(2\theta_2)\sin^2(\theta_2)-L_t\sin(\theta_s)+h_1\cos(\theta_s). \tag{7}$$

Figure 2(a) shows the angular aberration of the tandem parallel plate analyzer, $x_1(\theta)$ versus θ when $\theta_1=9°$, $\theta_2=13°$, $V_t/(q_sE_{p1})=1$ and Equation (4) is satisfied. The dashed curve shows the approximate curve utilizing Eq. (5). In Fig. 1(b) the calculated trajectories of the particle in the analyzer are shown when the incident angle is changed from 7° to 10° under the same parameters. In contrast to Fig. 2(a), the angular aberration of a usual parallel plate analyzer with $\theta_1=9°$ injection angle is shown in Fig. 2(b). It is clearly shown that the improvement in the aberration by a factor of several tens is obtained by the tandem analyzer by comparing Fig. 2(a) and 2(b). Figure 2(c) shows the energy dispersion of the tandem parallel plate analyzer $(\frac{\delta x_1}{\delta V_t})$ and the energy dispersions of the second stage of the analyzer under the assumption that the energy is changed only at the second stage. The dispersion is somewhat reduced due to the negative contribution at the first stage of the analyzer.

In conclusion, it is shown that a parallel plate analyzer has the second-order focus at arbitrary injection angle by a simple modification. This analyzer may be useful for the precise measurement of particles in MeV range, since the upper plate voltage can be enough low for high voltage breakdown by adopting low injection angle to the analyzer.

We would like to thank Director A. Iiyoshi and Professor M. Fujiwara for their continuous supports.

Reference

1) G. A. Harrower, Rev. Sci. Instrum. **26**, 850 (1955).

2) T. S. Green and G. A. Proca, Rev. Sci. Instrum. **41**,1409 (1970).

3) P. E. McLaren, K. A. Connor, J. F. Lewis, R. L. Hickok, T. P. Crowley, J. G. Schatz and G. H. Vilardi, Rev. Sci. Instrum. **61**,2955 (1990).

4) A. Fujisawa, H. Iguchi, A. Taniike, M. Sasao and Y. Hamada, Transactions on Plasma Science, **22**, 395 (1994).

Figure Captions

Figure 1(a). Schematics of a parallel plate analyzer. 1(b). Schematic view of a tandem parallel analyzer. The trajectories of the particle are calculated and shown at the second-order focus condition. $\theta_1 = 9°$, $\theta_2 = 13°$. $V_t/(q_s E_{p1}) = 1$ and Equation (4) is satisfied. The incident angle is changed from 7° to 10° by 1°.

Figure 2. Characteristics of the tandem parallel plate analyzer. 2(a). The angular aberration of the tandem parallel plate analyzer, $x_1(\theta)$ versus θ when $\theta_1 = 9°$, $\theta_2 = 13°$. $V_t/(q_s E_{p1}) = 1$. Equation (4) is satisfied. x_1 is the distance from the corner to the focus point, as is shown in Fig. 1(b). Equation (3) is calculated near the second-order focal point. The dashed curve shows the approximate curve utilizing Eq. (5). 2(b). The angular aberration of a usual parallel-plate analyzer with the injection angle of 9°. Equation (1) is calculated near the focal point. $V_t/(q_s E_{p1}) = 1$ is assumed. 2(c) shows the energy dispersion of the parallel plate analyzer. The

dashed curve shows the dispersion due to the second-stage of the analyzer.

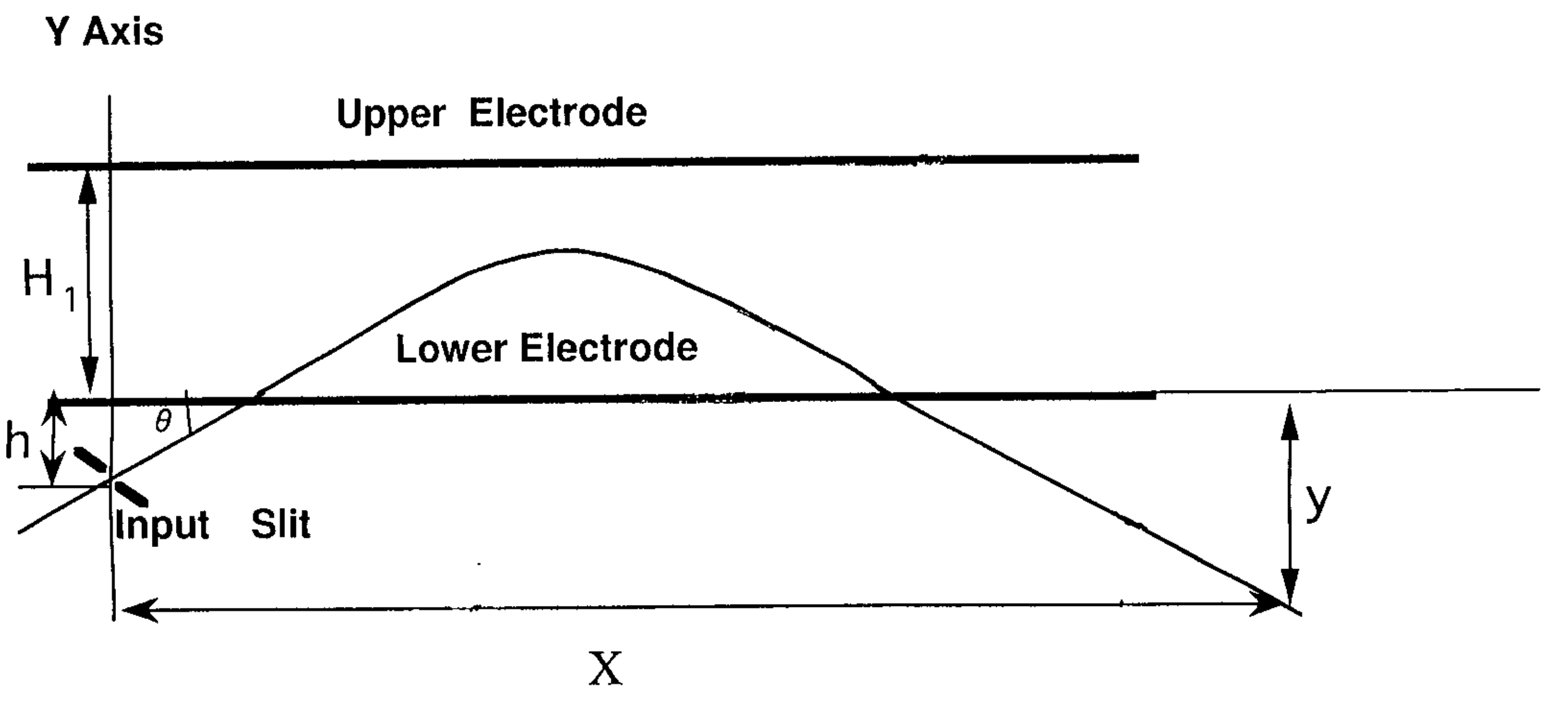

Figure 1(a)

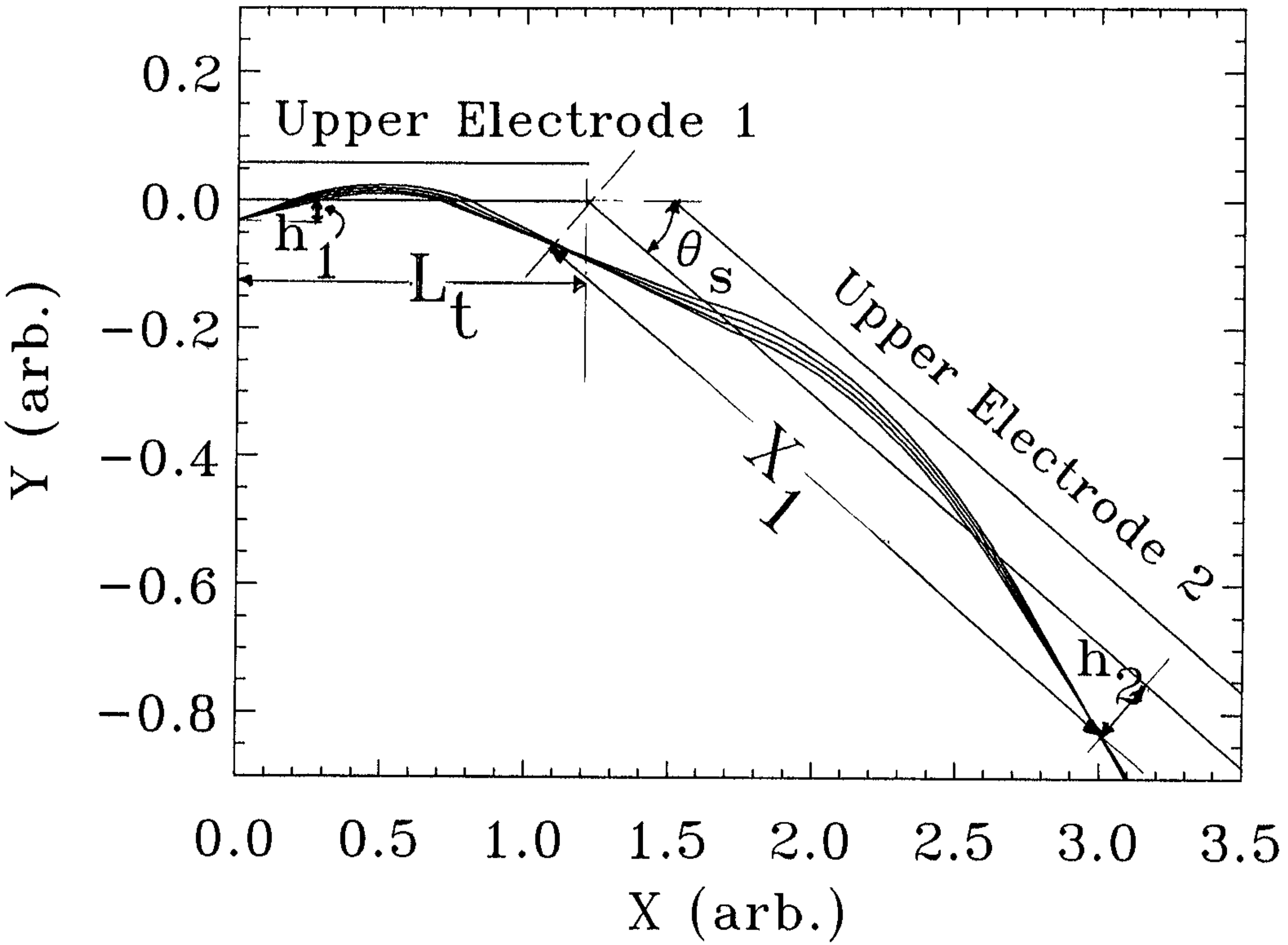
Upper Electrode 1
Upper Electrode 2
h_1
L_t
θ_s
X_1
h_2
0.2
0.0
−0.2
−0.4
−0.6
−0.8
Y (arb.)
0.0
0.5
1.0
1.5
2.0
2.5
3.0
3.5
X (arb.)

Fig. 1(b)

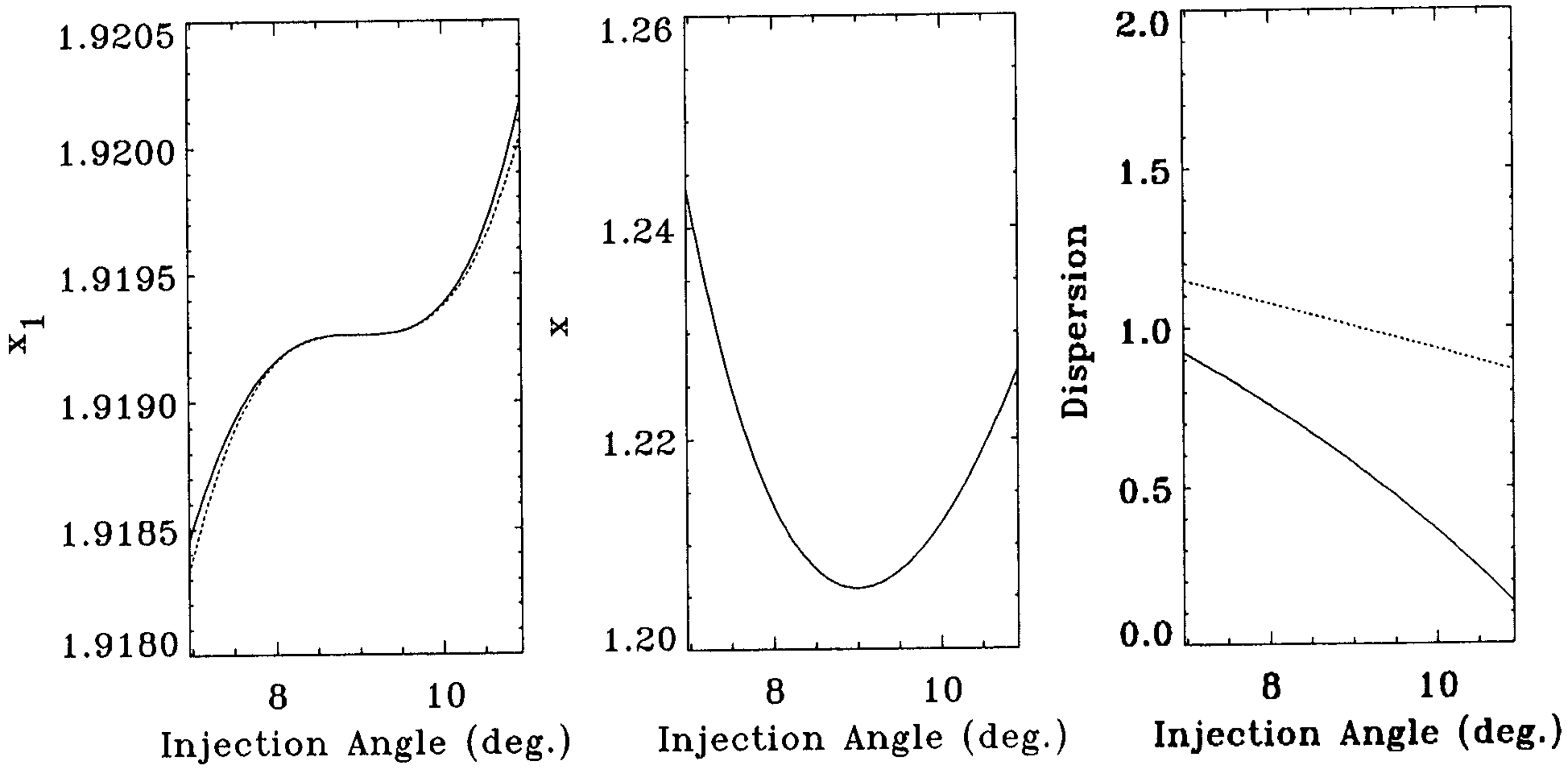
x_1
1.9205
1.9200
1.9195
1.9190
1.9185
1.9180
8
10
Injection Angle (deg.)
x
1.26
1.24
1.22
1.20
8
10
Injection Angle (deg.)
Dispersion
2.0
1.5
1.0
0.5
0.0
8
10
Injection Angle (deg.)

(a) (b) (c)

Figure 2

Recent Issues of NIFS Series

NIFS-422 Y. Kondoh, M. Yamaguchi and K. Yokozuka,
Simulations of Toroidal Current Drive without External Magnetic Helicity Injection; July 1996

NIFS-423 Joong-San Koog,
Development of an Imaging VUV Monochromator in Normal Incidence Region; July 1996

NIFS-424 K. Orito,
A New Technique Based on the Transformation of Variables for Nonlinear Drift and Rossby Vortices; July 1996

NIFS-425 A. Fujisawa, H. Iguchi, S. Lee, T.P. Crowley, Y. Hamada, H. Sanuki, K. Itoh, S. Kubo, H. Idei, T. Minami, K. Tanaka, K. Ida, S. Nishimura, S. Hidekuma, M. Kojima, C. Takahashi, S. Okamura and K. Matsuoka,
Direct Observation of Potential Profiles with a 200keV Heavy Ion Beam Probe and Evaluation of Loss Cone Structure in Toroidal Helical Plasmas on the Compact Helical System; July 1996

NIFS-426 H. Kitauchi, K. Araki and S. Kida,
Flow Structure of Thermal Convection in a Rotating Spherical Shell; July 1996

NIFS-427 S. Kida and S. Goto,
Lagrangian Direct-interaction Approximation for Homogeneous Isotropic Turbulence; July 1996

NIFS-428 V.Yu. Sergeev, K.V. Khlopenkov, B.V. Kuteev, S. Sudo, K. Kondo, F. Sano, H. Zushi, H. Okada, S. Besshou, T. Mizuuchi, K. Nagasaki, Y. Kurimoto and T. Obiki,
Recent Experiments on Li Pellet Injection into Heliotron E; Aug. 1996

NIFS-429 N. Noda, V. Philipps and R. Neu,
A Review of Recent Experiments on W and High Z Materials as Plasma-Facing Components in Magnetic Fusion Devices; Aug. 1996

NIFS-430 R.L. Tobler, A. Nishimura and J. Yamamoto,
Design-Relevant Mechanical Properties of 316-Type Stainless Steels for Superconducting Magnets; Aug. 1996

NIFS-431 K. Tsuzuki, M. Natsir, N. Inoue, A. Sagara, N. Noda, O. Motojima, T. Mochizuki, T. Hino and T. Yamashina,
Hydrogen Absorption Behavior into Boron Films by Glow Discharges in Hydrogen and Helium; Aug. 1996

NIFS-432 T.-H. Watanabe, T. Sato and T. Hayashi, *Magnetohydrodynamic Simulation on Co- and Counter-helicity Merging of Spheromaks and Driven Magnetic Reconnection*; Aug. 1996

NIFS-433 R. Horiuchi and T. Sato,
Particle Simulation Study of Collisionless Driven Reconnection in a Sheared Magnetic Field; Aug. 1996

NIFS-434 Y. Suzuki, K. Kusano and K. Nishikawa,
Three-Dimensional Simulation Study of the Magnetohydrodynamic Relaxation Process in the Solar Corona. II.; Aug. 1996

NIFS-435 H. Sugama and W. Horton,
Transport Processes and Entropy Production in Toroidally Rotating Plasmas with Electrostatic Turbulence; Aug. 1996

NIFS-436 T. Kato, E. Rachlew-Källne, P. Hörling and K.-D Zastrow,
Observations and Modelling of Line Intensity Ratios of OV Multiplet Lines for 2s3s 3S1 - 2s3p 3Pj; Aug. 1996

NIFS-437 T. Morisaki, A. Komori, R. Akiyama, H. Idei, H. Iguchi, N. Inoue, Y. Kawai, S. Kubo, S. Masuzaki, K. Matsuoka, T. Minami, S. Morita, N. Noda, N. Ohyabu, S. Okamura, M. Osakabe, H. Suzuki, K. Tanaka, C. Takahashi, H. Yamada, I. Yamada and O. Motojima,
Experimental Study of Edge Plasma Structure in Various Discharges on Compact Helical System; Aug. 1996

NIFS-438 A. Komori, N. Ohyabu, S. Masuzaki, T. Morisaki, H. Suzuki, C. Takahashi, S. Sakakibara, K. Watanabe, T. Watanabe, T. Minami, S. Morita, K. Tanaka, S. Ohdachi, S. Kubo, N. Inoue, H. Yamada, K. Nishimura, S. Okamura, K. Matsuoka, O. Motojima, M. Fujiwara, A. Iiyoshi, C. C. Klepper, J.F. Lyon, A.C. England, D.E. Greenwood, D.K. Lee, D.R. Overbey, J.A. Rome, D.E. Schechter and C.T. Wilson,
Edge Plasma Control by a Local Island Divertor in the Compact Helical System; Sep. 1996 (IAEA-CN-64/C1-2)

NIFS-439 K. Ida, K. Kondo, K. Nagaski T. Hamada, H. Zushi, S. Hidekuma, F. Sano, T. Mizuuchi, H. Okada, S. Besshou, H. Funaba, Y. Kurimoto, K. Watanabe and T. Obiki,
Dynamics of Ion Temperature in Heliotron-E; Sep. 1996 (IAEA-CN-64/CP-5)

NIFS-440 S. Morita, H. Idei, H. Iguchi, S. Kubo, K. Matsuoka, T. Minami, S. Okamura, T. Ozaki, K. Tanaka, K. Toi, R. Akiyama, A. Ejiri, A. Fujisawa, M. Fujiwara, M. Goto, K. Ida, N. Inoue, A. Komori, R. Kumazawa, S. Masuzaki, T. Morisaki, S. Muto, K. Narihara, K. Nishimura, I. Nomura, S. Ohdachi, M.. Osakabe, A. Sagara, Y. Shirai, H. Suzuki, C. Takahashi, K. Tsumori, T. Watari, H. Yamada and I. Yamada,
A Study on Density Profile and Density Limit of NBI Plasmas in CHS; Sep. 1996 (IAEA-CN-64/CP-3)

NIFS-441 O. Kaneko, Y. Takeiri, K. Tsumori, Y. Oka, M. Osakabe, R. Akiyama, T. Kawamoto, E. Asano and T. Kuroda,
Development of Negative-Ion-Based Neutral Beam Injector for the Large Helical Device; Sep. 1996 (IAEA-CN-64/GP-9)

NIFS-442 K. Toi, K.N. Sato, Y. Hamada, S. Ohdachi, H. Sakakita, A Nishizawa, A. Ejiri, K. Narihara, H. Kuramoto, Y. Kawasumi, S. Kubo, T. Seki, K. Kitachi, J. Xu, K. Ida, K. Kawahata, I. Nomura, K. Adachi, R. Akiyama, A. Fujisawa, J. Fujita, N. Hiraki, S. Hidekuma, S. Hirokura, H. Idei, T. Ido, H. Iguchi, K. Iwasaki, M. Isobe, O. Kaneko, Y. Kano, M. Kojima, J. Koog, R. Kumazawa, T. Kuroda, J. Li, R. Liang, T. Minami, S. Morita, K. Ohkubo, Y. Oka, S. Okajima, M. Osakabe, Y. Sakawa, M. Sasao, K. Sato, T. Shimpo, T. Shoji, H. Sugai, T. Watari, I. Yamada and K. Yamauti,
Studies of Perturbative Plasma Transport, Ice Pellet Ablation and Sawtooth Phenomena in the JIPP T-IIU Tokamak; Sep. 1996 (IAEA-CN-64/A6-5)

NIFS-443 Y. Todo, T. Sato and The Complexity Simulation Group,
Vlasov-MHD and Particle-MHD Simulations of the Toroidal Alfvén Eigenmode; Sep. 1996 (IAEA-CN-64/D2-3)

NIFS-444 A. Fujisawa, S. Kubo, H. Iguchi, H. Idei, T. Minami, H. Sanuki, K. Itoh, S. Okamura, K. Matsuoka, K. Tanaka, S. Lee, M. Kojima, T.P. Crowley, Y. Hamada, M. Iwase, H. Nagasaki, H. Suzuki, N. Inoue, R. Akiyama, M. Osakabe, S. Morita, C. Takahashi, S. Muto, A. Ejiri, K. Ida, S. Nishimura, K. Narihara, I. Yamada, K. Toi, S. Ohdachi, T. Ozaki, A. Komori, K. Nishimura, S. Hidekuma, K. Ohkubo, D.A. Rasmussen, J.B. Wilgen, M. Murakami, T. Watari and M. Fujiwara,
An Experimental Study of Plasma Confinement and Heating Efficiency through the Potential Profile Measurements with a Heavy Ion Beam Probe in the Compact Helical System; Sep. 1996 (IAEA-CN-64/C1-5)

NIFS-445 O. Motojima, N. Yanagi, S. Imagawa, K. Takahata, S. Yamada, A. Iwamoto, H. Chikaraishi, S. Kitagawa, R. Maekawa, S. Masuzaki, T. Mito, T. Morisaki, A. Nishimura, S. Sakakibara, S. Satoh, T. Satow, H. Tamura, S. Tanahashi, K. Watanabe, S. Yamaguchi, J. Yamamoto, M.Fujiwara and A. Iiyoshi,
Superconducting Magnet Design and Construction of LHD; Sep. 1996 (IAEA-CN-64/G2-4)

NIFS-446 S. Murakami, N. Nakajima, S. Okamura, M. Okamoto and U. Gasparino,
Orbit Effects of Energetic Particles on the Reachable β–Value and the Radial Electric Field in NBI and ECR Heated Heliotron Plasmas; Sep. 1996 (IAEA-CN-64/CP -6) Sep. 1996

NIFS-447 K. Yamazaki, A. Sagara, O. Motojima, M. Fujiwara, T. Amano, H. Chikaraishi, S. Imagawa, T. Muroga, N. Noda, N. Ohyabu, T. Satow, J.F. Wang, K.Y. Watanabe, J. Yamamoto , H. Yamanishi, A. Kohyama, H. Matsui, O. Mitarai, T. Noda, A.A. Shishkin, S. Tanaka and T. Terai
Design Assessment of Heliotron Reactor; Sep. 1996 (IAEA-CN-64/G1-5)

NIFS-448 M. Ozaki, T. Sato and the Complexity Simulation Group, *Interactions of Convecting Magnetic Loops and Arcades*; Sep. 1996

NIFS-449 T. Aoki,
Interpolated Differential Operator (IDO) Scheme for Solving Partial Differential Equations; Sep. 1996

NIFS-450 D. Biskamp and T. Sato,
Partial Reconnection in the Sawtooth Collapse; Sep. 1996

NIFS-451 J. Li, X. Gong, L. Luo, F.X. Yin, N. Noda, B. Wan, W. Xu, X. Gao, F. Yin, J.G. Jiang, Z. Wu., J.Y. Zhao, M. Wu, S. Liu and Y. Han,
Effects of High Z Probe on Plasma Behavior in HT-6M Tokamak; Sep. 1996

NIFS-452 N. Nakajima, K. Ichiguchi, M. Okamoto and R.L. Dewar,
Ballooning Modes in Heliotrons/Torsatrons; Sep. 1996 (IAEA-CN-64/D3-6)

NIFS-453 A. Iiyoshi,
Overview of Helical Systems; Sep. 1996 (IAEA-CN-64/O1-7)

NIFS-454 S. Saito, Y. Nomura, K. Hirose and Y.H. Ichikawa,
Separatrix Reconnection and Periodic Orbit Annihilation in the Harper Map; Oct. 1996

NIFS-455 K. Ichiguchi, N. Nakajima and M. Okamoto,
Topics on MHD Equilibrium and Stability in Heliotron / Torsatron; Oct. 1996

NIFS-456 G. Kawahara, S. Kida, M. Tanaka and S. Yanase,
Wrap, Tilt and Stretch of Vorticity Lines around a Strong Straight Vortex Tube in a Simple Shear Flow; Oct. 1996

NIFS-457 K. Itoh, S.- I. Itoh, A. Fukuyama and M. Yagi,
Turbulent Transport and Structural Transition in Confined Plasmas; Oct. 1996

NIFS-458 A. Kageyama and T. Sato,
Generation Mechanism of a Dipole Field by a Magnetohydrodynamic Dynamo; Oct. 1996

NIFS-459 K. Araki, J. Mizushima and S. Yanase,
The Non-axisymmetric Instability of the Wide-Gap Spherical Couette Flow; Oct. 1996

NIFS-460 Y. Hamada, A. Fujisawa, H. Iguchi, A. Nishizawa and Y. Kawasumi,
A Tandem Parallel Plate Analyzer; Nov. 1996